JOURNAL OF MATERIALS SCIENCE 24 (1989) 1089–1094

The formation of zinc ferrite

F. J. C. M. TOOLENAAR
Philips Research Laboratories, PO Box 80 000 5600 JA Eindhoven, The Netherlands

The formation of zinc ferrite from zinc oxide and iron oxide is evaluated with high temperature X-ray diffraction experiments. Despite the problem of accurately determining the temperature of the part of the sample actually investigated, a kinetic analysis of the isothermal formation is shown to be possible. From these data the energy and entropy of activation are derived. It is further shown that neither corrections for grain growth during formation nor the presence of impurities have any influence on these results. On the other hand, the size of the reactant iron oxide particles is found to have a strong influence on both the energy and entropy of activation.

1. Introduction

Often the processing of even long established products like ferrites is only poorly understood and hence imperfectly controlled. For instance, the chemical composition of samples during processing at elevated temperatures, like calculating or sintering, is usually unknown. Sometimes quenching is applied as a method to obtain the (frozen-in) situation at a high temperature, but this is accompanied by some obvious disadvantages:

(i) It is difficult to exclude fully the possibility of changes during cooling.

(ii) Each quenching experiment produces only one point on a temperature-time scale.

In principle, high temperature X-ray diffraction (HTXRD) offers a means to investigate variations in chemical composition, but care should be taken with the following points:

(i) It is difficult to obtain quantitative results.

(ii) Only a relatively small surface layer of the sample is covered.

(iii) At high temperatures no additional changes should occur (e.g. in preferential exposure of lattice planes or in particle size) which would influence the relative intensities.

In a previous investigation [1] into the reactive sintering of zinc ferrite (i.e. the simultaneous occurrence of formation reaction and densification), we reported a small but distinct difference in the formation temperature depending on the type of iron oxide applied. In Fig. 1 these results are reproduced. The objective of this investigation was to link this difference with possible variations in (apparent) thermodynamic quantities.

2. Quantitative analysis of X-ray diffractograms

The intensity of an X-ray diffraction line from a particular lattice plane of a chemical species is dependent not only on the number of absorbing elements, but also on its mass absorption coefficient as well as on that of the matrix [2]. In a first approximation the observed intensity of a single component i in a mixture of n different species can be expressed as

$$\frac{I_i}{I_i^0} = \frac{x_i \mu_i^*}{\sum_{i=1}^{n} x_i \mu_i^*} \tag{1}$$

where I_i is the observed intensity, I_i^0 the intensity in a matrix of pure i, x_i is the weight fraction and μ_i^* the mass absorption coefficient of species i. For $n = 3$ this leads to

$$\frac{I_1}{I_2}\frac{I_2^0}{I_1^0} = \frac{x_1 \mu_1^*}{x_2 \mu_2^*} \tag{2}$$

and

$$\frac{I_1}{I_3}\frac{I_3^0}{I_1^0} = \frac{x_1 \mu_1^*}{x_3 \mu_3^*} = \frac{x_1 \mu_1^*}{(1 - x_1 - x_2)\mu_3^*} \tag{3}$$

if we define

$$c_{ij} \equiv \frac{\mu_i^*}{\mu_j^*}\frac{I_i^0}{I_j^0} \tag{4}$$

it follows that

$$x_2 = x_1 \frac{\mu_1^*}{\mu_2^*}\frac{I_1^0}{I_2^0}\frac{I_2}{I_1} = x_1 c_{12}\frac{I_2}{I_1}$$

Introduction into Equation 3 leads to

$$x_1 = \left(1 - x_1 - x_1 c_{12}\frac{I_2}{I_1}\right) c_{31}\frac{I_1}{I_3}$$

By definition $c_{12}c_{31} = c_{32}$ and thus

$$x_1 = \frac{c_{31} I_1}{c_{31} I_1 + c_{32} I_2 + I_3}$$

or, more generally:

$$x_i = \frac{c_n I_i}{\sum_{i=1}^{n} c_{ni} I_i} \tag{5}$$

Theoretically, therefore, one would only need the diffractograms of the pure substances to derive the concentration of any one of them in a mixture. In practice, however, it is advisable to check the thus determined c values with calibration mixtures. Note that this calibration is performed at room temperature and

0022–2461/89 $03.00 + .12

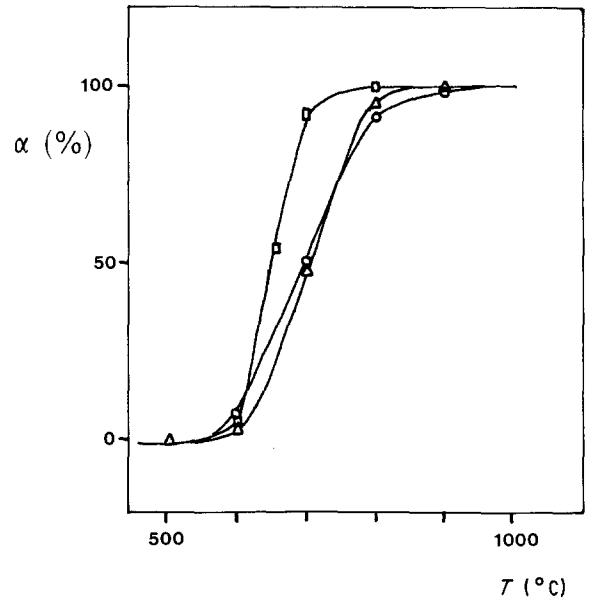

Figure 1 Zinc ferrite conversion in sintered pellets (from [1]). The curves indicate the non-calcined mixtures of UCB zinc oxide with: BASF iron oxide (○), calcined BASF iron oxide (△) or Ruthner Hoogovens iron oxide (□).

that disturbing effects at high temperatures are not accounted for in this way.

3. Experimental details

Just as before [1], non-calcined mixtures of ZnO (from UCB, Union Chimique Belgique) and one of the following types of iron oxide were used: BASF, the same calcined in air at 800° C, or a Ruthner type from Hoogovens. The codes of the respective mixtures are (A), (B) and (C). In Table I the relevant data of the raw materials are reproduced [1].

The pellets for the HTXRD investigations were made as thin as possible to facilitate the heat flow, but thick enough to be selfsupporting without a binder. In practice they had a thickness of 1.00 ± 0.05 mm and a diameter of 10 mm.

For quantitative analysis calibration mixtures were prepared as follows. The pure constituents were calcined in an appropriate atmosphere at 800° C and

TABLE I Raw materials

	ZnO	Fe_2O_3[1]		
		a	b	c
A ($m^2 g^{-1}$)[2]	3	20	2.5	3
D_N (μm)[3]	0.4	0.06	0.5	0.4
Purity[4]	99.99	99.96	99.96	99.5
Na	< 0.01	< 0.01	< 0.01	0.02
Si	< 0.001	0.002	0.003	0.009[5]
Ca	< 0.001	< 0.001	< 0.001	0.009
Mn	0.0001	0.01	0.01	0.2
Ni	< 0.001	0.002	0.002	0.03
Cl	< 0.001	< 0.001	< 0.001	0.085

[1] a: BASF iron oxide
b: BASF iron oxide calcined at 700° C in air
c: Ruthner iron oxide
[2] Specific surface area from BET
[3] Particle size from A
[4] By spectrochemical analysis in wt % (unless otherwise indicated)
[5] By chemical analysis in wt %

TABLE II X-ray peaks applied

Substance	*hkl*	I/I_1	*d*	$(2\theta)_{CuK\alpha}$
ZnO	102	29	1.91	47.6
Fe_2O_3	024	40	1.84	49.6
$ZnFe_2O_4$	422	12	1.72	53.3

subsequently ball-milled to obtain a comparable particle size. Accurately weighed amounts were then mixed for 10 min in a type MS (Retsch) spectro-mill.

The measuring device consisted of a Philips PW 1050 powder diffractometer equipped with an HTXRD set-up (MRC), using Cu$K\alpha$ radiation. The HTXRD set-up consisted essentially of a platinum foil which could be resistively heated to about 1400° C. The temperature was measured with a (Pt/Pt–10% Rh) thermocouple attached to the bottom of the foil. The sample was glued to the top of the foil with a normal commercial adhesive, which was burned out during the experiment. All experiments described in this paper were carried out in air.

For the determination of the conversion α of zinc oxide and iron oxide into zinc ferrite a part of the diffractogram had to be scanned which contained non-interfering peaks of the three substances. Such a part was found between 46 and 56° (2θ) see Table II. However, due to the limited scanning speed, the number of points that could be collected as a function of time, would have been too small, for example, to detect the presence of a linear relationship at the start of an experiment. The following experimental procedure was adopted therefore. During the first 10 min only the (422)-spinel peak was monitored at a rate of $1° min^{-1}$. Then the part of the diffractogram containing all three peaks was scanned at a rate of $2° min^{-1}$. With these diffractograms the conversion α was determined from the relative peak heights; the conversion in the first 10 min was then determined by interpolation.

4. Results

The X-ray data of the peaks applied in this investigation are collected in Table II. The relevant results of the calibration are given in Table III. The calibration constants were determined directly from the values of the mass absorption coefficients of the individual atoms (for Cu$K\alpha$ radiation): $\mu^*_{ZnO} = 51$, $\mu^*_{Fe_2O_3} = 219$ and $\mu^*_{ZnFe_2O_4} = 162$ and from measurements of the pure materials: $I^0_{ZnO} = 13800$ cps, $I^0_{Fe_2O_3} = 2480$ cps, $I^0_{ZnFe_2O_4} = 2020$ cps.

With Equation 4 one finds: $c_{SZ} = 0.46$ and $c_{SF} = 0.60$, with Z, F and S defined as in Table III. The absorption coefficient of the mixture $\mu^*_{tot.} = \Sigma^n_{i=1} x_i \mu^*_i$ should be constant, which proved to be true within 1%. Results of the application of the calibration constants to the calibration mixtures are given in Table III, indicating satisfactory results.

The conversion into zinc ferrite was investigated by isothermal runs of all three mixtures. The conversion in each case was determined as described above. The results are shown in Fig. 2, showing the onset of the reaction. By plotting the data as a function of the logarithm of time (Fig. 3), the course of the conversion over a longer period can be observed.

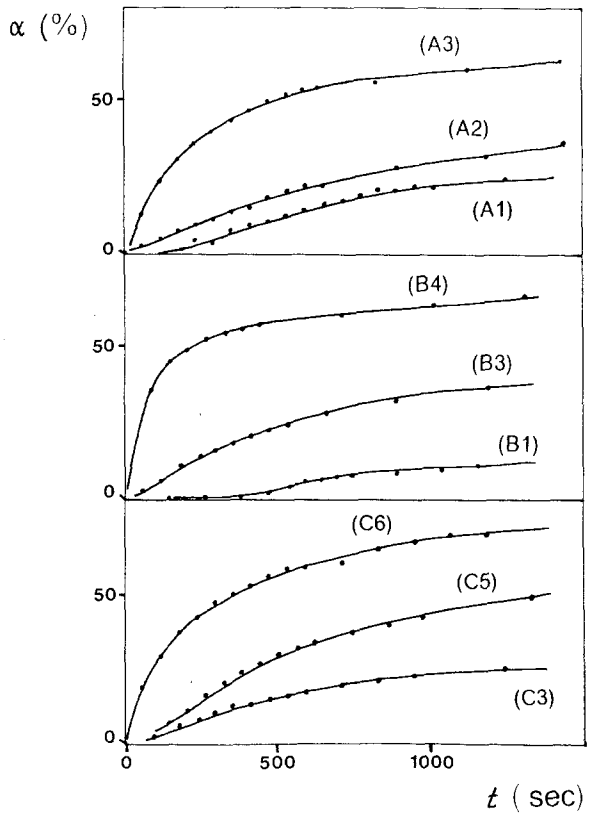

Figure 2 Zinc ferrite conversion as a function of time in the first stages of the process; the experiment numbers (cf. Table IV) are indicated.

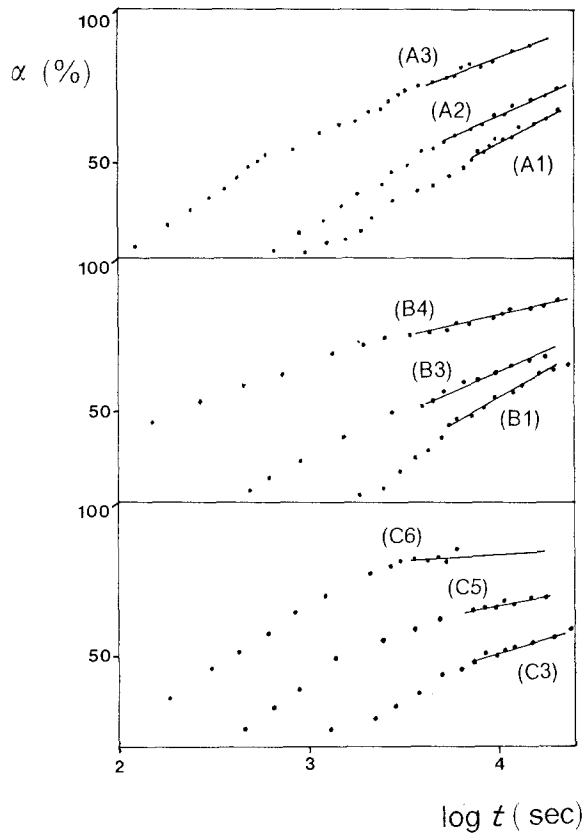

Figure 3 Zinc ferrite conversion as a function of the logarithm of time; the experiment numbers (cf. Table IV) are indicated. The conversion after 4 h (log t = 4.16) can easily be obtained by interpolation.

5. Evaluation and discussion

The conversion as a function of time (Fig. 2) for each isothermal run shows that the reaction is continuously decelerated, following approximately a parabolic rate law. This is to be expected for a diffusion-controlled reaction. At the start, however, the curves show a sigmoid behaviour, which would indicate that kinetic control is exerted by nuclei growth.

The results of the ferrite formation of all mixtures as a function of temperature (Fig. 2) first appeared to be very unreproducible. In fact, it turned out that the temperature in the region investigated with X-ray diffraction was not simply related to that of the platinum support foil. As the thickness of the samples varied only marginally, the most likely cause lies in the contact between sample and platinum foil. Apparently, the method of attaching the sample to the platinum was not reproducible.

Nevertheless, an evaluation of the kinetics proved possible with the help of an external "calibration". The idea was to compare the conversion α after 4 h in the present experiments with that in a pellet which has been sintered for 4 h in a conventional furnace with accurate temperature control. In Fig. 3 it is shown that a plot of the conversion data from the present experiments against the logarithm of the time resulted in more or less straight lines. The conversion after 4 h, determined by interpolation was then compared with the experimentally found relation [1] between conversion and sinter temperature (see Fig. 1). From this figure, the "real" temperature was derived and further used in the investigation. The results for the three mixtures in this investigation are collected in Table IV.

In the literature, usually a function of α is plotted against (the logarithm of) time. This is based on a model of the chemical reaction proceeding in a powdered, i.e. not continuous, compact. The original

TABLE III Calibration

Mixture	Weighed in (%)[1]			Intensity (cps)[1]			Intensity (%)[1,2]		
	Z	F	S	Z	F	S	Z	F	S
1	34	66	0	1540	2200	0	35	65	0
2	28	54	18	1300	1840	380	29	53	18
3	22	43	35	880	1440	780	20	42	38
4	16	31	53	600	1020	1080	14	31	55
5	10	19	71	370	660	1430	9	20	71
6	3.5	7.5	89	140	260	1820	3	8	89

[1] Z = ZnO; F = Fe_2O_3; S = $ZnFe_2O_4$

[2] Obtained from the experimental intensities by multiplying by the calibration contants, c_{SZ} = 0.46 and c_{SF} = 0.60, determined from measurements of the pure substances.

TABLE IV Evaluation of the reaction rate constants

Exp.[1]	t[2]	T_x[3]	T_c[4]	$10^3/T_c$[5]	ln k_J[6]	Γ[7]	ln k_{J_+}[8]	ln k_{C_+}[9]
(A1)	5200	700	728	0.999	−4.88	6.3	−3.03	−3.58
(A2)	3900	750	740	0.987	−4.24	6.7	−2.42	−2.97
(A3)	600	800	790	0.941	−2.41	8.3	−0.37	−1.06
(B1)	6000	750	715	1.012	−4.98	1.6	−4.62	−5.29
(B2)	3100	800	722	1.005	−4.54	1.5	−4.10	−4.64
(B3)	1800	850	730	0.997	−3.96	1.4	−3.67	−4.02
(B4)	450	900	760	0.968	−2.21	1.1	−1.77	−2.21
(C1)	11000	725	635	1.101	−6.84	1.6	−6.36	−7.04
(C2)	11000	700	640	1.095	−6.13	1.6	−5.70	−6.13
(C3)	3200	750	660	1.072	−5.04	1.4	−4.61	−5.25
(C4)	3600	775	670	1.060	−4.25	1.5	−3.84	−4.45
(C5)	1500	750	675	1.055	−3.42	1.3	−3.24	−3.94
(C6)	600	800	690	1.038	−2.22	1.1	−2.12	−2.75

[1]The experiment number, in which the letters indicate the mixture of UCB zinc oxide with:
A: BASF iron oxide;
B: calcined BASF iron oxide;
C: Ruthner Hoogovens iron oxide.
[2]The time interval (in sec.) over which the function J (eq. 6) varies linearly with time (see Fig. 4).
[3]The temperature (in °C) measured with the thermocouple connected to the platinum foil.
[4]The temperature in the pellet (in °C) deduced from the conversion after 4 h.
[5]ln K^{-1}
[6]The logarithm of the Jander rate constant in $ksec^{-1}$
[7]The correction factor for grain growth (Equation 7).
[8]The logarithm of the Jander rate constant (in $ksec^{-1}$) corrected for grain growth (Equation 7).
[9]The logarithm of the Carter rate constant (in $ksec^{-1}$) corrected for grain growth (Equation 8).

description was given by Jander [3] as follows. The rate of formation of a product layer with thickness y in a spheroidal particle is

$$\frac{dy}{dt} = \frac{k}{y} \rightarrow y^2 = 2kt$$

where k is a constant. The volume of material which has not yet reacted is

$$V = \tfrac{4}{3}\pi(r_0 - y)^3 = \tfrac{4}{3}\pi r_0^3(1 - x)$$

where r_0 is the particle radius and x is the fraction which has reacted. From this it follows that

$$y = r_0[1 - (1 - x)^{1/3}]$$

This results in

$$J = [1 - (1 - x)^{1/3}]^2 = \frac{2kt}{r_0^2} \qquad (6)$$

the Jander equation. A plot of J against t should result in a straight line. In Fig. 4 the results of our experiments show that a linear relationship can indeed be detected in the first part of the experiments*. The deviations from linearity are probably caused by a more rapid completion of the reaction in the smallest particles, thus reducing the total number of particles participating in the reaction. The rate constants are now obtained directly from the slopes of these straight lines and are shown in Table IV as k_J.

However, this may actually be done only if the particle size r_0 is a real constant. This is not so in our experiments: a linear relationship between the average particle size (or in fact: the specific surface area) and the logarithm of time has been observed in sintered pellets [1]. Although such a correction should in fact be entered before the derivation of Equation 6, it was entered in a first approximation as follows†:

$$k_{J_+} = k_J\left[\Delta\left(\frac{r}{r_0}\right)\frac{\ln t}{\ln 14400}\right]^2 = k_J\Gamma^\dagger \qquad (7)$$

where $\Delta(r/r_0)$ is the ratio of grain size increase after 4 h and t is the time during which the Jander equation is obeyed linearly. The logarithms of the thus corrected rate constants are shown in Table IV as ln k_{J_+}.

In later years several authors have suggested improvements of Jander's theory. For instance, Cater [4] argued that equalizing the sphere volumes to obtain the relationship between x and y can only be justified if no volume change occurs by the reaction. By introducing z, the volume of product formed per unit volume of original reactant consumed, he arrived at the following equation

$$C = [1 + (z - 1)x]^{2/3} + (z - 1)(1 - x)^{2/3}$$
$$= z + 2(1 - z)kt/r_0^2 \qquad (8)$$

Taking $z = 1.48$, the molar volume ratio of $ZnFe_2O_4$ and Fe_2O_3, a plot of C against t also results in a linear relationship (Fig. 5). From the slopes of these lines again a set of k values is obtained; the logarithms of these constants, after a correction for coarsening, are shown in Table III as k_{C_+}.

From the reaction rate theory [5] the rate constant of a chemical reaction is

$$k = \frac{k_B T}{h}\exp(\Delta S^\dagger/R)\exp(-\Delta H^\dagger/RT)$$

*Note that this linearity could not have been observed if full diffractograms had been recorded, resulting in time intervals of at least 5 min.
†The reference time of no grain growth is arbitrarily taken as 1 sec.

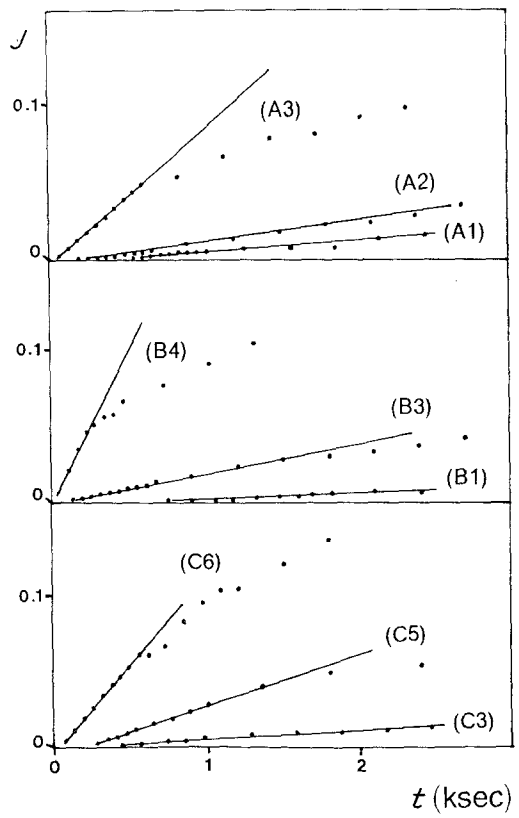

Figure 4 The Jander plot (Equation 6); the experiment numbers (cf. Table IV) are indicated.

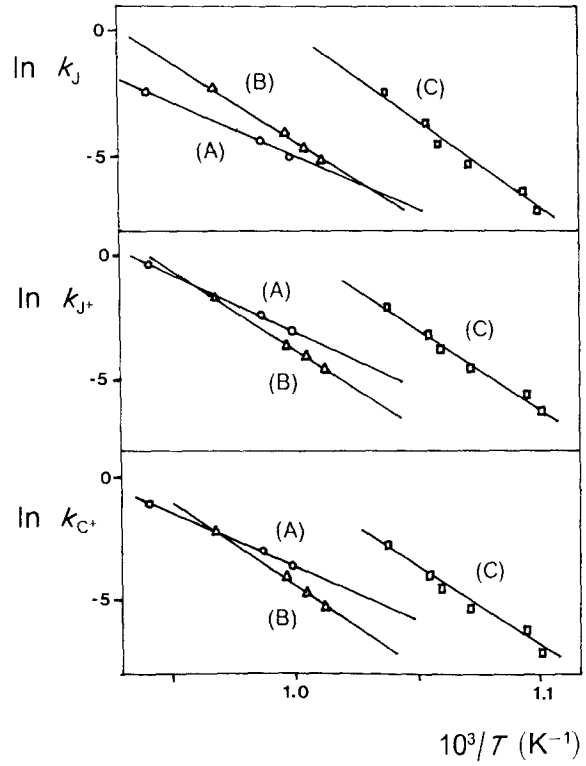

Figure 6 Arrhenius plot with the various rate constants (data from Table IV; evaluation in Table V).

or

$$\ln k = \ln\left(\frac{k_B T}{h}\right) + \frac{\Delta S^\dagger}{R} - \frac{\Delta H^\dagger}{RT}, \qquad (9)$$

where k_B and h are the Boltzmann and Planck constants, $\Delta S^\dagger$ is the entropy, $\Delta H^\dagger$ the enthalpy of activation of the formation reaction. Between 600 and 800° C $\ln (k_B T/h) = 23.7 \pm 0.1\,\text{ksec}^{-1}$ and may therefore be regarded as independent of temperature. A plot of $\ln k$ against $1/T$ should then produce a straight line from which the thermodynamic functions may be calculated. The results are shown in Fig. 6. The data of these plots and the values of the thus derived thermodynamic functions are given in Table V. As can be seen, the coarsening correction appears to improve the (already acceptable) linearity of the plots, but does not have a substantial influence on the thermodynamic values. The same holds for applying the Carter equation. In fact no alternative description (like, e.g. that of Ginstling and Brounshtein [6]) was shown to give any improvement. Most likely, these refinements are only important when the particles are very large, as in model system investigations.

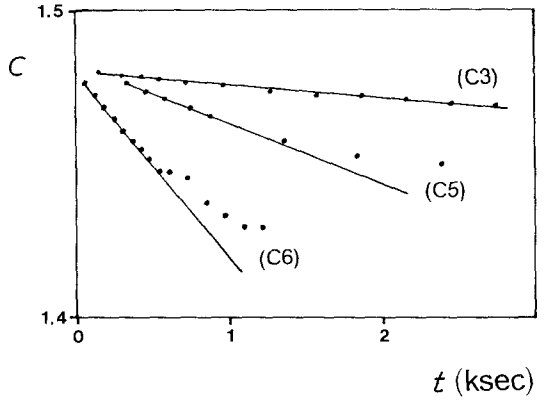

Figure 5 The Carter plot (Equation 8) for (C)-mixture experiments (cf. Table IV); note that the part of the experiment that has a linear dependency is not different from that obtained with the Jander formula (cf. Fig. 4).

The absolute values of thermodynamic parameters obtained in this way agree in order of magnitude with those found in literature. Duncan and Stewart [7], for example, found for the same reaction: $\Delta H^+ = 420\,\text{kJ mol}^{-1}$ and $\Delta S^\dagger = 117\,\text{J mol}^{-1}\,\text{K}^{-1}$. The reason for the fairly large spread of the values found in the

TABLE V The apparent thermodynamic functions

Mix[1]	k[2]	s_J[3]	i_J[4]	r[5]	$\Delta H^\dagger$[6]	$\Delta S^\dagger$[7]
(A)	k_J[8]	−41.8	36.9	0.9985	348	110
(B)		−62.9	58.7	0.9995	522	291
(C)		−70.1	70.3	0.9900	583	387
(A)	k_{J+}[9]	−45.5	42.4	0.9997	378	155
(B)		−64.2	60.4	0.9996	534	305
(C)		−64.6	64.8	0.9944	537	342
(A)	k_{C+}[10]	−42.9	39.3	0.9993	357	130
(B)		−68.3	64.0	0.9967	568	335
(C)		−63.1	62.6	0.9893	525	323

[1]The mixtures of UCB zinc oxide with:
(A): BASF iron oxide;
(B): calcined BASF iron oxide;
(C): Ruthner Hoogovens iron oxide.
[2]The rate constant applied (cf. Table 4).
[3]The slope of the $\ln k$ against $10^3/T$ curve in K sec^{-1}.
[4]The intercept in ksec^{-1}.
[5]The correlation coefficient by the least-squares method.
[6]The activation enthalpy $\Delta H^+ = -s_J R$ in kJ/mole (cf. Equation 9).
[7]The activation entropy ΔS^+ in J mol^{-1} K^{-1} (cf. Equation 9).
[8]The Jander rate constant (cf. Equation 6).
[9]The Jander rate constant corrected for grain growth (cf. Equation 7).
[10]The Carter rate constant corrected for grain growth (cf. Equation 8).

present experiments is no doubt at least partly caused by the rather indirect temperature registration. More interesting, however, are the (significant) differences found between the mixtures applied in this investigation. As expected, the results of the mixtures (A) and (C) did show a difference. However, (C) displayed a *larger* activation energy and entropy, which can hardly be seen as the reflection of a conversion at a lower temperature. Furthermore, the values obtained with (B) resembled the ones obtained with (C) and not those of (A). Obviously, the (apparent) thermodynamic parameters derived in this investigation are not linked with the temperature of the formation reaction, nor, for that matter, with the presence of impurities. It appears that they are determined by the morphology of the reactants. Apparently, the smaller iron oxide particles facilitate the proceeding of the formation reaction by their larger surface area.

6. Conclusions

(1) It is possible to obtain reliable kinetic data with HTXRD experiments, provided that the temperature of the investigated part of the material is accurately determined.

(2) The apparent thermodynamic parameters of the zinc ferrite formation reaction are strongly influenced by the morphology of the reactants; they are not linked with the formation temperature.

Acknowledgements

The author would like to thank A. M. Romijnders for preparative assistance and C. Langereis and H. C. A. M. Smoorenburg for performing the X-ray experiments.

References

1. F. J. C. M. TOOLENAAR and M. T. J. VERHEES, *J. Mater. Sci.* **23** (1988) 256.
2. H. P. KLUG and L. E. ALEXANDER, "X-ray Diffraction Procedures" (Wiley, New York, 1954).
3. W. JANDER, *Z. anorg. u. algem. Chem.* **163** (1927) 1.
4. R. E. CARTER, *J. Chem. Phys.* **34** (1961) 2010.
5. K. J. LAIDLER, "Chemical Kinetics" 2nd edn (McGraw-Hill, New York, 1965), p. 89.
6. A. M. GINSTLING and B. I. BROUNSHTEIN, *J. Appl. Chem. USSR* **23** (1950) 1327.
7. J. F. DUNCAN and D. J. STEWART, *Trans. Farad. Soc.* **63** (1967) 1031.

Received 18 January
and accepted 1 June 1988